Zeitschrift: Helvetica Physica Acta
Band: 66 (1993)
Heft: 6

Artikel: Selfgravitating solutions of the Skyrme model and their stability
Autor: Heusler, Markus / Straumann, Norbert / Zhou, Zhi-hong
DOI: https://doi.org/10.5169/seals-116583

Helv Phys Acta
Vol. 66 (1993)

0018-0238/93/060614-19$1.50+0.20/0

SELFGRAVITATING SOLUTIONS OF THE SKYRME MODEL AND THEIR STABILITY

Markus Heusler [†], Norbert Straumann and Zhi-hong Zhou [‡]

[†] Max-Planck-Institut für Astrophysik, Karl-Schwarzschild-Strasse 1,
D-8046 Garching bei München, Germany
[‡] Institut für Theoretische Physik, Universität Zürich, Schönberggasse 9,
CH-8001 Zürich, Switzerland
(24. VI. 1993)

Abstract

We give a brief survey of the spherically symmetric soliton and black hole solutions of the Einstein-Skyrme system, of which we have presented the fundamental branches in a recent publication. Some of the basic features and the linear stability properties of both classes of solutions are discussed. We also derive a mass variation formula for general stationary Skyrme black holes and show that the latter assumes the familiar vacuum form in the static, spherically symmetric case under consideration. We conclude with new results of a numerical non-linear stability analysis which yields strong evidence for the stability of the fundamental soliton solutions. Thus, contrary to the solutions of the Einstein-Yang-Mills system, all arguments indicate that the Einstein-Skyrme black holes represent stable counter examples to the no-hair conjecture.

1 Introduction

Recently it has become evident, that the coupling of gravitation to non-linear field theories results in many cases in a spectrum of classical solutions which is considerably richer than originally expected. Stimulated by the work of Bartnik and McKinnon [1], who found a gravitationally bound SU(2) Yang-Mills *soliton* solution, having no flat spacetime counterpart, plenty of work has been performed in this area.

Shortly after the discovery of the Bartnik-McKinnon (BK) solution, several authors have also constructed *black hole* solutions of the SU(2) Einstein-Yang-Mills (EYM) theory [2, 3, 4]. Although these (and the BK) solutions turned out to be unstable [5, 6, 7, 8], they remain interesting for several reasons, mainly because they shed new light on the famous no-hair conjecture for black holes. Their existence, which meanwhile has been established rigorously [9, 10], destroyed the widespread belief that (in addition to their mass and angular momentum) all stationary black holes are uniquely characterized by a set of global charges: The SU(2) black hole solutions have vanishing YM charges and asymptotically approach the Schwarzschild solution, but are completely different from the latter in the vicinity of the horizon. However, one might take the view that this does not contradict the no-hair conjecture, if the latter is restricted to *stable* configurations.

Among other reasons, it was mainly this objection which motivated us to look for black hole solutions of related selfgravitating non-linear field theories, hoping that these might exhibit *stable* hair. Promising candidates are non-linear σ-models coupled to gravity. As in the YM case, Derrick's theorem prohibits regular, finite energy configurations in flat spacetime, provided that one deals with the "minimal" version, i.e. with an action which is quadratic (harmonic) in the first derivatives of the matter fields. However, contrary to the YM case, it turns out that these models have neither soliton nor black hole solutions when gravity is "switched on". Using scaling arguments, we were able to prove the corresponding non-existence and no-hair theorems for spherically symmetric σ-models with harmonic action in [11, 12]. The proof of the general no-hair theorem for these models, which relies on the sole symmetry requirement of stationarity and makes essential use of the positive mass theorem, was recently given in [13].

As these no-go results demonstrate, one has to consider Einstein-σ-models with more general than quadratic matter actions in order to obtain interesting new solutions. An obvious possibility is given by the Skyrme model which exhibits soliton solutions even in flat space, as a result of an additional quartic term in the Lagrangian. The latter was introduced by Skyrme [14, 15] in order to describe mesons within an $SU(2) \times SU(2)$ invariant theory, which was later suggested to emerge in the low energy limit of QCD.

In this article we shall first summarize the results of our previous investigations on soliton and black hole solutions of the Einstein-Skyrme (ES) model and their linear stability [16, 17, 18]. Subsequently we shall present the results of a numerical analysis which yields strong evidence for the stability of the lowest energy ES solutions even under *non-linear* perturbations.

The paper is organized as follows. The second section is devoted to the derivation of the basic ES equations without imposing symmetries. It is shown that the Skyrme and Einstein

equations can be written in the form

$$(2fg)^2\, d*A + [A\,,\, d*(A\wedge A)] = 0\,, \qquad G_{\mu\nu} = 8\pi G(2\frac{\partial \mathcal{L}}{\partial g^{\mu\nu}} - \mathcal{L}\, g_{\mu\nu})\,,$$

respectively, where $\mathcal{L}$ denotes the Skyrme Lagrangian, f and g are coupling constants and $A = U^{\dagger}dU$, U denoting the $SU(2)$-valued function describing the π and σ fields.

In the third section, we shall evaluate these basic equations for time-dependent hedgehog configurations of the Skyrme field.

The main properties of the fundamental *static* regular and black hole solutions are summarized in the forth section. In addition, we present numerical evidence for the existence of two branches of asymptotically flat solutions in every topological sector. It is also shown that the number of topological sectors containing black hole or soliton solutions decreases with increasing coupling constant.

In the fifth section we show that the mass variation formula for static ES black holes is identical with the corresponding "first law" formula [19] for the Schwarzschild solution. This conclusion was first drawn by Zaslavskii from an explicit computation [20] and has recently been confirmed by some of us, using more general arguments [21].

The linear stability of the fundamental soliton and black hole solutions is discussed in the sixth section. We recall that it is possible to obtain the frequency spectrum of radial perturbations from the energy spectrum of a Schrödinger equation. It turns out that the properties of the effective potential are such that no bound states exist for the solutions of the lower energy branch. This guarantees the linear stability of both, the fundamental regular and the fundamental black hole solutions.

In the last section we shall present new results of a non-linear numerical perturbation analysis. Our investigations indicate that the selfgravitating (lower branch) Skyrme solutions are stable under non-linear perturbations.

2 The Field Equations

The physical motivation to consider the Skyrme model is based on the expectation that in the low-energy limit of QCD, bosons can be considered as soliton solutions of an effective non-linear σ-model Lagrangian (see e.g. [22]). Since Derrick's scaling argument excludes energetically stable regular solutions of minimal (i.e. quadratic action) σ-models, higher order derivative terms have to be taken into account. The simplest realization of this idea is represented by the $SU(2) \times SU(2)$ invariant Skyrme Lagrangian density [14, 15, 23, 24, 25]

$$\mathcal{L} = \frac{f^2}{4}\, tr\,(\nabla_\mu U \nabla^\mu U^{\dagger}) + \frac{1}{32g^2}\, tr\,([\nabla_\mu U\, U^{\dagger}\,,\, \nabla_\nu U\, U^{\dagger}]^2)\,, \tag{1}$$

where ∇ denotes the covariant derivative with respect to the spacetime metric, g is the dimensionless (rho meson / pionic current) coupling constant, f is the pion decay constant ($f \cong 190\, MeV$), and $U = U(x)$ denotes the $SU(2)$-valued function describing the meson fields. It is very convenient to rewrite the Skyrme Lagrangian in terms of the 1-form A, defined as the pull-back $U^*(\theta)$ of the Maurer-Cartan form θ of $SU(2)$. As a consequence of the Maurer-Cartan equation, A satisfies the identity

$$dA + A \wedge A = 0\,. \tag{2}$$

Using

$$A = U^{\dagger} dU\,, \quad F := A \wedge A\,, \tag{3}$$

one immediately finds from (1)

$$\mathcal{L}\eta = -\frac{f^2}{4} tr\,(A \wedge *A) + \frac{1}{16g^2} tr\,(F \wedge *F)\,, \tag{4}$$

where $\eta = *1$ is the volume 4-form, $*$ denotes the Hodge dual and $A \wedge *A = (A|A)\eta = A_\mu A^\mu \eta$, $F \wedge *F = (F|F)\eta = (1/2)F_{\mu\nu}F^{\mu\nu}\eta$. The variations of the two contributions in the action integral can be transformed to

$$\frac{1}{2}\delta\, tr\,(A \wedge *A) = -tr\,(U^{\dagger}\delta U\; d * A\,) + d(...)\,, \tag{5}$$

$$\frac{1}{2}\delta\, tr\,(F \wedge *F) = tr\,(U^{\dagger}\delta U\,[A\,, d * F]\,) + d(...)\,. \tag{6}$$

This yields the following compact form of the Skyrme equations:

$$(2fg)^2\; d * A + [A\,, d * F] = 0\,. \tag{7}$$

In the derivation of the identities (5) and (6) one makes use of $\delta A = U^{\dagger}(d(\delta U) - (\delta U)A)$, well-known properties of the Hodge dual and the general relations

$$[\alpha, \beta] = \alpha \wedge \beta - (-1)^{pq}\,\beta \wedge \alpha\,,$$

$$tr\,(\alpha \wedge \beta) = (-1)^{pq}\, tr\,(\beta \wedge \alpha)\,,$$

which hold for arbitrary p- and q-forms α and β, respectively.

In addition to the Skyrme equation (7) we also have Einstein's equations, describing the back reaction of the matter to the gravitational field. Since the Lagrangian (4) does not depend on derivatives of the metric, the energy momentum tensor is given by

$$T_{\mu\nu} = 2\,\frac{\partial \mathcal{L}}{\partial g^{\mu\nu}} - \mathcal{L}\, g_{\mu\nu}\,, \tag{8}$$

which immediately yields the Einstein equations

$$G_{\mu\nu} = \kappa\, tr\,(-[A_\mu A_\nu - \frac{1}{2}(A|A)g_{\mu\nu}] + (2gf)^{-2}\,[F_{\mu\rho}F_{\nu}{}^{\rho} - \frac{1}{2}(F|F)g_{\mu\nu}])\,. \tag{9}$$

Here we have introduced the dimensionless coupling constant κ [16],

$$\kappa = 4\pi\,(\frac{f}{m_{Pl}})^2\,, \tag{10}$$

where m_{Pl} denotes the Planck mass.

3 Selfgravitating Hedgehog Configurations

Since we are interested in the stability of spherically symmetric black hole and soliton solutions, we restrict ourselves to the well-known hedgehog ansatz [24, 26]

$$U = \cos\chi(r,t) + i\,\tau_r \sin\chi(r,t)\,, \tag{11}$$

where the angular field variable χ depends on the radial coordinate r and in general also on the time t. It is convenient to use the spherical SU(2) generators τ_r, τ_ϑ and τ_φ,

$$\tau_r = \vec{\tau}\,\hat{r}\,, \quad \tau_\vartheta = \partial_\vartheta\,\tau_r\,, \quad \tau_\varphi = \sin^{-1}\vartheta\,\partial_\varphi\,\tau_r\,, \tag{12}$$

which satisfy the usual commutator relations $[\tau_r,\tau_\vartheta] = 2i\,\tau_\varphi$, cycl.. With respect to the orthonormal frame of 1-forms $\{\theta^\mu\}$, defined as

$$\theta^0 = e^a\,dt\,, \quad \theta^1 = e^b\,dr\,, \quad \theta^2 = r\,d\vartheta\,, \quad \theta^3 = r\sin\vartheta\,d\varphi\,, \tag{13}$$

one finds the following expressions for A and F in terms of $a(r,t)$, $b(r,t)$ and $\chi(r,t)$

$$-i\,A = \chi_{,t}\,\tau_r\,e^{-a}\theta^0 + \chi_{,r}\,\tau_r\,e^{-b}\theta^1 + \frac{\sin\chi}{r}\,(\tau_s\theta^2 + \tau_c\theta^3)\,, \tag{14}$$

$$-i\,F = 2\,\frac{\sin\chi}{r}\,[(\tau_c\theta^2 - \tau_s\theta^3)\wedge(\chi_{,t}\,e^{-a}\theta^0 + \chi_{,r}\,e^{-b}\theta^1)] - 2\,(\frac{\sin\chi}{r})^2\,\tau_r\theta^2\wedge\theta^3\,, \tag{15}$$

where $\tau_s := \sin\chi\tau_\varphi + \cos\chi\tau_\vartheta$, $\tau_c := \cos\chi\tau_\varphi - \sin\chi\tau_\vartheta$ (and hence $[\tau_s,\tau_c] = 2i\,\tau_r$, cycl.). Introducing the dimensionless coordinates x and τ and the functions u and v [17],

$$x = g\,f\,r\,, \quad \tau = g\,f\,t\,, \tag{16}$$

$$u = x^2 + 2\sin^2\chi\,, \quad v = \sin^2\chi\,(2 + \frac{\sin^2\chi}{x^2})\,, \tag{17}$$

the action integrand (4) becomes

$$\mathcal{L}\,\eta = \frac{f^2}{4}\,[\,e^{b-a}\,u\,(\dot{\chi})^2 - e^{a-b}\,u\,(\chi')^2 - e^{a+b}\,v\,]\,dr\wedge dt\wedge d\Omega\,, \tag{18}$$

where the dot and the dash denote the partial derivatives with respect to τ and to x, respectively. Using the expressions (14) and (15) for A and F, the Skyrme equations (7) reduce to a second order equation for $\chi(x,\tau)$ and the Einstein equations (9) give three first order equations for $a(x,\tau)$ and $b(x,\tau)$:

$$(e^{b-a}\,u\dot{\chi})^{\cdot} - (e^{a-b}\,u\chi')' - \frac{u_\chi}{2}\,[e^{b-a}\,(\dot{\chi})^2 - e^{a-b}\,(\chi')^2] + \frac{v_\chi}{2}\,e^{a+b} = 0\,, \tag{19}$$

$$1 - e^{-2b}\,(1 - 2xb') = \kappa\,[v + u\,(e^{-2a}\,(\dot{\chi})^2 + e^{-2b}\,(\chi')^2)]\,, \tag{20}$$

$$1 - e^{-2b}\,(1 + 2xa') = \kappa\,[v - u\,(e^{-2a}\,(\dot{\chi})^2 + e^{-2b}\,(\chi')^2)]\,, \tag{21}$$

$$\dot{b} = \kappa\,\frac{u}{x}\,\dot{\chi}\,\chi'\,. \tag{22}$$

Here u' and u_χ denote the total derivative with respect to x and the partial derivative with respect to χ, respectively.

4 Static Soliton and Black Hole Solutions

In the static case, the Skyrme equation (19) and the remaining two Einstein equations (20) and (21) assume the form

$$(e^{-\delta} N u \chi')' = \frac{1}{2} e^{-\delta} (N u_\chi (\chi')^2 + v_\chi), \tag{23}$$

$$\mu' = \kappa \frac{1}{2} (N u (\chi')^2 + v), \tag{24}$$

$$\delta' = -\kappa \frac{u}{x} (\chi')^2, \tag{25}$$

where we have introduced the dimensionless mass μ and replaced the metric functions a and b by μ and δ,

$$e^{-2b} = N = 1 - \frac{2\mu}{x}, \quad \delta = -(a + b). \tag{26}$$

(Note that both μ and δ are constant for the Schwarzschild solution.) In addition, we obtain the effective static matter Lagrangian from (18),

$$\mathcal{L}_m = \frac{\kappa}{2} e^{-\delta} (N u (\chi')^2 + v). \tag{27}$$

It can immediately be verified that the static, spherically symmetric field equations (23)-(25) are obtained as the Euler-Lagrange equations of the effective matter plus gravitation Lagrangian $\mathcal{L}_{eff}(\mu, \mu', \delta, \delta', \chi, \chi')$ [11],

$$\mathcal{L}_{eff} = \mathcal{L}_m + \mathcal{L}_g, \text{ where } \mathcal{L}_g = -\mu' e^{-\delta}. \tag{28}$$

The requirement of asymptotic flatness dictates the following boundary conditions for μ, δ and χ as $x \to \infty$:

$$\mu(\infty) = \text{const.}, \quad \delta(\infty) = \text{const.}, \quad \chi(\infty) = -k_\infty \pi, \quad (x^2 \chi')(\infty) = 0. \tag{29}$$

In [16] we have numerically investigated both, the lowest energy asymptotically flat soliton and black hole solutions of the system (23)-(25).

Regular solutions: The first class of solutions generalizes the flat Skyrme solitons to the selfgravitating case. The regularity conditions at the center $x = 0$ imply

$$\mu(0) = \mu'(0) = \mu''(0) = 0, \quad \delta'(0) = 0, \quad \chi(0) = \pi, \tag{30}$$

and soliton solutions are found by adjusting the only free parameter $\chi'(0)$ such that the boundary conditions (29) and (30) are fulfilled. (Note that the ambiguity of $\delta(0)$ only reflects a gauge-freedom.) As we have demonstrated in [16] for the lowest topological sector $k_\infty = 0$, this is possible for all coupling constants κ below a critical maximal value $\kappa_{max} \cong 0.0404$. As a matter of fact, for every $\kappa < \kappa_{\max}$ one finds a *pair* of soliton solutions, coinciding for $\kappa = \kappa_{\max}$. For $\kappa > \kappa_{\max}$ there are no regular solutions satisfying the boundary conditions at the center *and* at infinity. A similar kind of behavior is also found in the higher topological sectors ($k_\infty > 0$), where the bifurcation value κ_{max} at which the two branches coincide decreases with increasing k_∞.

As in flat spacetime, $\chi(\infty) = -k_\infty \pi$ implies that 3-space can be compactified and $U(x)$ becomes a map from S^3 to $SU(2)$. Up to a sign, the pull-back of the normalized invariant volume-form on $SU(2)$ is

$$\omega = \frac{1}{24\,\pi^2}\, tr\,(A \wedge A \wedge A)\,, \tag{31}$$

and the integral of $-\omega$ is thus equal to the winding number $n = 1 + k_\infty$ of the map U, $\Pi^3(SU(3)) = \mathcal{Z}$. One immediately obtains this result from the expressions (14) and (15) with $\chi_{,t} = 0$, since

$$tr\,(A \wedge F) = 12\, r^2 e^{-b}\, \sin^2(\chi)\, \chi_{,r}\; \theta^1 \wedge \theta^2 \wedge \theta^3\,, \tag{32}$$

and hence, using $2\sin^2(\chi)\chi_{,r}\, dr = d(\chi + \sin(\chi)\cos(\chi))$,

$$n = -\int \omega = \frac{1}{4\pi^2} \int_{\chi(0)}^{\chi(\infty)} d\,(\chi + \sin(\chi)\cos(\chi))\, d\Omega = 1 + k_\infty\,. \tag{33}$$

Black holes: The second class of asymptotically flat solutions of the hedgehog ES equations (23)-(25) are characterized by the existence of a regular event horizon $\mathcal{H}$ at $x = x_h$, where

$$N(x_h) = 0 \quad \Longleftrightarrow \quad \mu(x_h) = \frac{1}{2}\, x_h\,. \tag{34}$$

In order to construct solutions which are regular for $x \geq x_h$, one now has to impose the horizon boundary conditions

$$\mu'(x_h) = \frac{\kappa}{2}\{v\}_{x_h}\,, \quad \delta'(x_h) = -\kappa\,\{\frac{u}{x}(\chi')^2\}_{x_h}\,, \quad \chi'(x_h) = \{\frac{x\, v_\chi}{2u(1-\kappa v)}\}_{x_h}\,, \tag{35}$$

which reflects the fact that the power series of μ, δ and χ in the vicinity of the horizon are now determined by the parameter $\chi(x_h)$. For a given value of the coupling constant κ and the horizon distance x_h, $\chi(x_h)$ has to be adjusted such that the solution satisfies the asymptotic flatness conditions (29). In the lowest sector ($k_\infty = 0$) this turns out to be possible only for $\kappa \leq \kappa_{max}(x_h)$, where, like in the regular case, one finds again a *pair* of solutions. In addition, to every value of $\kappa \leq \kappa_{max}$ there belongs a maximal horizon value $x_h^{max}(\kappa)$, beyond which no black hole solutions can exist. $x_h^{max}(\kappa)$ takes its maximal value for $\kappa \to 0$ ($x_h^{max}(0) \cong 0.1238$) and shrinks monotonically to zero as κ increases to the critical value. (In [11] we have also given an analytic proof for the existence of the maximal horizon distance $x_h^{max}(\kappa)$. The existence of a maximal κ-value is immediately obtained from the horizon boundary conditions (35).)

The behavior described above repeats itself in the higher topological sectors ($k_\infty > 0$). As in the soliton case, the critical value $\kappa_{max}(x_h)$ decreases when k_∞ is increased (for a fixed value of x_h).

Fig. 1a shows the hedgehog field $\chi(x)$ and the mass function $\mu(x)$ of a fundamental (i.e. lower branch) and its corresponding upper branch black hole solution in the lowest topological sector $k_\infty = 0$. The same quantities are plotted in Fig. 1b for the pair of solutions in the second topological sector $k_\infty = 1$, where the parameters κ and x_h are the same as in Fig. 1a. In Fig. 2 we have plotted the "shooting parameter" $\chi(x_h)$ as a function of the coupling constant κ (for a fixed value of x_h) for the solutions in the first ($k_\infty = 0$) and

second ($k_\infty = 1$) sector. The figure illustrates that the branches converge at the bifurcation point $\kappa_{max}(x_h)$, whose value decreases with increasing k_∞. (Note also that for all upper energy branches $\chi(x_h) > \pi/2$ as $\kappa \to 0$.) It is finally worth pointing out that it is sufficient to consider solutions with $\chi(x_h) \in]\pi/2, \pi[$ and $k_\infty \geq 0$, since the differential equations (23)-(25) are invariant with respect to reflections at $\pi/2$, $\chi \to \pi - \chi$ and to translations $\chi \to \chi + p\pi$ (with integer p). Fig. 3 gives an overview on the asymptotic behavior of generic solutions with $\chi(x_h) \in]\pi/2, \pi[$, among which the asymptotically flat black hole solutions (integer k_∞) represent a discrete set.

Although we have classified the black hole solutions according to the value of k_∞, they are, contrary to the soliton solutions, topologically trivial, since $\chi(x_h) = \pi$ would force $\chi(x) =$ const. for all x. Hence, the ES black holes provide counter examples to the expectation that only static black hole solutions of selfgravitating matter models with *non-vanishing* asymptotic charges differ from the Schwarzschild solution. Moreover, since all investigations indicate that the lower branch black holes are stable, these also violate the weakened version of the no-hair conjecture, according to which any *stable* black hole solution should be uniquely characterized by a set of global quantities defined at spacelike infinity.

5 The Mass Variation Formula

Following the traditional reasoning of Bardeen, Carter and Hawking [19, 27], we have recently established the following mass and mass variation formulae for stationary black holes with matter Lagrangian $\mathcal{L}$ [21] (asuumed to be independent on derivatives of the metric):

$$M = \frac{1}{4\pi}\kappa_{\mathcal{H}} A_{\mathcal{H}} + 2\Omega_{\mathcal{H}} J_{\mathcal{H}} + 4\int_\Sigma *\mathcal{L}_g(k) + 2\int_\Sigma (\mathcal{L} - tr(\mathcal{L}_g)) * k\,, \tag{36}$$

$$\delta M = \frac{1}{8\pi}\kappa_{\mathcal{H}}\,\delta A_{\mathcal{H}} + \Omega_{\mathcal{H}}\,\delta J_{\mathcal{H}} + 2\delta\int_\Sigma *\mathcal{L}_g(k) - \delta_U\int_\Sigma \mathcal{L} * k\,, \tag{37}$$

where $\kappa_{\mathcal{H}}$, $A_{\mathcal{H}}$, $\Omega_{\mathcal{H}}$ and $J_{\mathcal{H}}$ denote the surface gravity, the area, the angular velocity and the angular momentum of the horizon, respectively. Furthermore, we have introduced the notation $(\mathcal{L}_g)_{\mu\nu} = \partial\mathcal{L}/\partial g^{\mu\nu}$, $(\mathcal{L}_g(k))_\mu = (\mathcal{L}_g)_{\mu\nu}k^\nu$ and the symbols δ and δ_U to denote general variations and variations with respect to the matter fields, respectively. Here we are interested in non-rotating solutions $\Omega_{\mathcal{H}} = 0$. For a theory with stationary scalar fields, this already implies staticity [13] which means that the timelike Killing field (1-form) k is hypersurface orthogonal. Using the stationarity condition $L_k U = 0$ for the Skyrme field we obtain $L_k A = L_k F = 0$ for the Lie derivatives with respect to k and hence $\mathcal{L}_g(k) = 0$. Making use of the Euler-Lagrange (Skyrme) equations, the remaining integral in the mass variation formula (37) can be converted into a boundary integral (see [21] for details). This finally yields the formulae

$$M = \frac{1}{4\pi}\kappa A + 2E_S\,, \tag{38}$$

$$\delta M = \frac{1}{8\pi}\kappa\,\delta A - \int_{\partial\Sigma} tr\,(\delta U * (k \wedge \mathcal{L}_{dU}))\,, \tag{39}$$

where E_S is the volume energy contribution of the Skyrme part of the Lagrangian,

$$E_S = \frac{1}{16g^2}\int_\Sigma tr\,(F|F)\,(-*k)\,. \tag{40}$$

A scaling argument shows [11] that the Skyrme contribution E_S to the total mass is equal to the contribution of the harmonic term, $E_H = (f^2/4)\int_\Sigma tr(A|A)(-*k)$, implying that

$$M = \frac{1}{4\pi}\kappa A + E(U), \tag{41}$$

with $E(U) = E_H + E_S$. As a consequence of the general properties of Killing horizons and the invariance of the Skyrme field U under the action of k, the horizon part of the boundary integral in (39) vanishes (cf. [21]). Hence, the only additional contribution to the vacuum mass variation formula can possibly arise from a boundary term at infinity. However, it is immediately seen that the asymptotic flatness conditions (29) imply that this term vanishes as well, since

$$tr\,[\delta U * (k \wedge \mathcal{L}_{dU})] \propto \chi' x^2\, d\Omega \to 0, \quad \text{for } x \to \infty. \tag{42}$$

This demonstrates that the "first law" of black hole thermodynamics assumes the same form for both, the Schwarzschild and the hedgehog Skyrme black holes with hair [20, 21]:

$$\delta M = \frac{1}{8\pi}\kappa\,\delta A. \tag{43}$$

6 Linear Stability

The linear (Ljapunov) stability of the lower branch regular ($n = 1$) and black hole ES solutions was analyzed in [17] and [18]. It was shown that Einstein's equations can be used to eliminate the radial metric perturbations δa and δb for a wide class of matter models. This procedure yields the Schrödinger equation

$$[-\frac{d^2}{d\rho^2} + V(\rho)]\,\zeta(\rho) = \sigma^2\,\zeta(\rho), \tag{44}$$

with the effective potential $V(\rho)$, which is determined by the static solution χ, N, δ. The amplitude $\zeta(\rho)$ is defined in terms of $u = x^2 + 2\sin^2\chi$ and the perturbation $\delta\chi$ of the Skyrme field as

$$\zeta(x) = \sqrt{u}\,\delta\chi(x,\tau)\,e^{-i\sigma\tau}, \tag{45}$$

where the new coordinate ρ is obtained from the dimensionless radial coordinate x by solving the differential equation

$$\frac{d\rho}{dx} = e^{\delta(x)}\,N^{-1}(x). \tag{46}$$

In the regular case, where $N(0) = 1$ (and $\delta(0) := 0$), ρ is a radial coordinate with $\rho(0) = 0$, and the effective potential V has the form

$$V(\rho) = \tilde{V}(\rho) + \frac{2}{\rho^2}, \tag{47}$$

where $\tilde{V}(\rho)$ is smooth and bounded for $\rho \geq 0$. In order to find the number of (exponentially growing) unstable modes one has to determine the spectrum of the Schrödinger equation (44) with potential (47), i.e. to investigate the number of p-wave bound state of $\tilde{V}(\rho)$. This

can be done by applying Levinson's theorem [28, 29]. A numerical investigation then shows that no such bound states exist in the case under consideration [17]. This establishes the linear stability of selfgravitating lower energy branch Skyrme solitons. It should also be noted that the numerical analysis becomes unreliable if the coupling constant is very close to the critical value κ_{max}. This is due to the existence of the second, unstable upper branch of $k_\infty = 0$ solutions, coinciding with the stable one for $\kappa = \kappa_{max}$ [30].

In the case of the black hole solutions, the horizon boundary condition $N(x_h) = 0$ and the differential equation (46) together imply that ρ maps the domain $]x_h, \infty[$ outside the horizon to the entire real axis. Thus, the eigenvalue equation (44) has to be solved on the whole real line. As we have demonstrated in [18], the effective potential $V(\rho)$ is bounded and fulfills $V(\rho = \pm\infty) = 0$. A detailed numerical study shows that the Schrödinger equation has no bound states for all values of x_h and κ which allow for lower branch black hole solutions. (It should be emphasized, that the negativity of the minimum of V does *not* necessarily indicate the existence of a bound state of the Schrödinger equation on $]-\infty, \infty[$.) Hence, the fundamental black hole solutions with Skyrme hair are linearly stable under radial perturbations.

7 Nonlinear Numerical Stability Analysis

Linear stability is a necessary but not sufficient condition for the stability of a soliton or a black hole solution. Once it is established one is actually in an extremely difficult situation, even for the corresponding problem for finite dynamical systems. (We recall that the stability problem for a linearly stable equilibrium configuration of a Hamiltonian system with more than two degrees of freedom is still far from being solved.) All we can do at this point is to study numerically the evolution of some representative perturbations. For obvious reasons we carried this out only for the regular solutions.

For a numerical study it is convenient to rewrite the basic equations (19) - (22) in first order form. Introducing the quantity

$$\pi = e^{b-a}\, u\dot{\chi}, \tag{48}$$

one finds the following system of equations:

$$\dot{\pi} = e^{-\delta}\{N\,[u\chi'' + 2x\chi' + \frac{u_\chi}{2}(\frac{\pi^2}{u^2} + (\chi')^2)] + [\frac{u\chi'}{x^2}\,(2m - \kappa x v) - \frac{v_\chi}{2}]\}\,, \tag{49}$$

$$\dot{\chi} = e^{-\delta}\frac{N}{u}\pi\,, \tag{50}$$

$$\dot{\mu} = \kappa N^2 e^{-\delta}\pi\chi'\,, \tag{51}$$

$$\delta' = -\frac{\kappa}{x}(\frac{\pi^2}{u} + u(\chi')^2)\,, \tag{52}$$

$$\mu' = \frac{\kappa}{2}(v + N(\frac{\pi^2}{u} + u(\chi')^2))\,, \tag{53}$$

where the definitions (26) of δ and μ are kept in the time dependent case.

The corresponding Cauchy problem is well defined; one has to give initial values for χ and π. The initial data for the metric functions δ and μ are then determined by eqs. (52) and (53), together with appropriate boundary conditions ($\mu(0) = 0$, $\delta(\infty) = 0$). The first three equations (49)–(51) then predict χ, π and μ at an infinitesimally later time. Subsequently, the corresponding metric function δ is determined by eq. (52), where the Hamiltonian constraint (53) is automatically satisfied. This propagating constraint equation provides in fact an important and useful check for the accuracy of our numerically constructed solutions.

We applied the MacCormack algorithm to solve the above equations. However, a 4-point forward-backward difference scheme was used in our simulations instead of the 2-point scheme in the standard MacCormack algorithm. We conducted many tests on our code, such as running static solutions, changing time and space steps, and so on. We will not describe the details of the algorithm and code tests in this paper but refer the reader to [8] and references therein. In all simulations, the Hamiltonian constraint was monitored and required to be satisfied with an accuracy better than 10^{-4}.

To start the simulation, we superposed a Gaussian perturbation on a static solution, i.e.

$$\chi(x, t_0) = \chi^{\alpha}_{st}(x, \kappa) + Ae^{-B(x-C)^2} \tag{54}$$

where χ_{st} stands for the static soliton solution. For a given sector (k_∞) we distinguish the two branches by an index $\alpha \in \{s, u\}$, where s denotes the lower (linearly stable) and u the upper (linearly unstable) mass branch, respectively. A, B, and C are three free parameters. In the figures presented below, the perturbation width B is always chosen to be 4.0 and for C we take the value 1.5 (but many different combinations of the parameters were also simulated). The function π is initially set to zero. The initial values of δ and μ are then determined by eqs. (52) and (53) with the boundary conditions $\mu(0) = 0$ and $\delta(\infty) = 0$.

We first ran simulations for the linearly stable lower energy branch soliton (for a typical coupling constant $\kappa = 0.02$). The results are shown in Figs. 4a and 4b, where the amplitudes of the perturbations are 0.3 and -0.3, respectively. The absolute value of the amplitude is quite large compared to $\chi^s_{st}(x = C, \kappa = 0.02) = 0.68$. Under these perturbations the total initial dimensionless mass, $\mathcal{M} = \mu(\infty)$, rises from the static one, $\mathcal{M}_{st} = 0.108$, to $\mathcal{M} = 0.115$ (for $A = 0.3$) and to $\mathcal{M} = 0.114$ (for $A = -0.3$). The mass increase is thus about 6%. From Figs. 4a and 4b we can see that the initial perturbations are quickly damped and then propagate outwards roughly at the speed of light, independently of the sign of the perturbation. The outgoing waves carry away the extra energy of the initial perturbations. The perturbed solitons then settle down to the static solution. This is also seen from Fig. 5 where the dimensionless mass functions are plotted at different times. A closer look shows that the total mass decreases to 0.108 at later times, which is just the static mass for $\kappa = 0.02$. In Fig. 6 we present the perturbed mass function together with the one of the equilibrium solution. One sees clearly that the perturbed soliton indeed returns to equilibrium. We conclude that the lower energy branch solitons are stable with respect to these perturbations.

The picture emerging from simulations with $\kappa = 0.04$ is quite different, as can be seen from Figs. 7a and 7b. The initial perturbations are no longer damped as quickly as for $\kappa = 0.02$. Instead they oscillate, at least in the range our simulations can cover. This is due to the fact that $\kappa = 0.04$ is very close to the bifurcation value $\kappa_{max} \cong 0.0404$ ($x_h = 0.02$) , at which the unstable upper branch solution coincides with the lower energy solution.

We also ran simulations for the linearly unstable branch. We perturbed the soliton χ^u_{st} ($\kappa = 0.02$) with amplitude $A = 0.2$. The results are presented in Figs. 8a and 8b. Fig. 8a shows the time evolution of $\chi - \chi^s_{st}$. In Fig. 8b we plot the field variable χ for the perturbed unstable soliton at $t = 0$ (solid line) and at $t = 40$ (dashed line) and compare it with χ^u_{st} (dotted line) and with χ^s_{st} (squares). From these figures it becomes obvious that the perturbed unstable soliton approaches the lower energy solution (and stays there). This result confirms the instability of the upper branch solitons χ^u_{st} and demonstrates also that the lower branch solutions χ^s_{st} are indeed stable.

We did not exhaust all reasonable perturbations (it is always possible to construct very large perturbations which break the soliton), but the simulations we carried out show no sign that the perturbed fundamental soliton might collapse or dissolve, in contrast to what happens for the EYM solitons [7, 8]. Thus, our simulations give strong evidence that the selfgravitating Skyrme solitons are stable. From this we expect that the black hole solutions are also stable. Clearly it is very difficult to show this, which becomes evident from the fact that the corresponding problem has not even been solved for the Schwarzschild black hole.

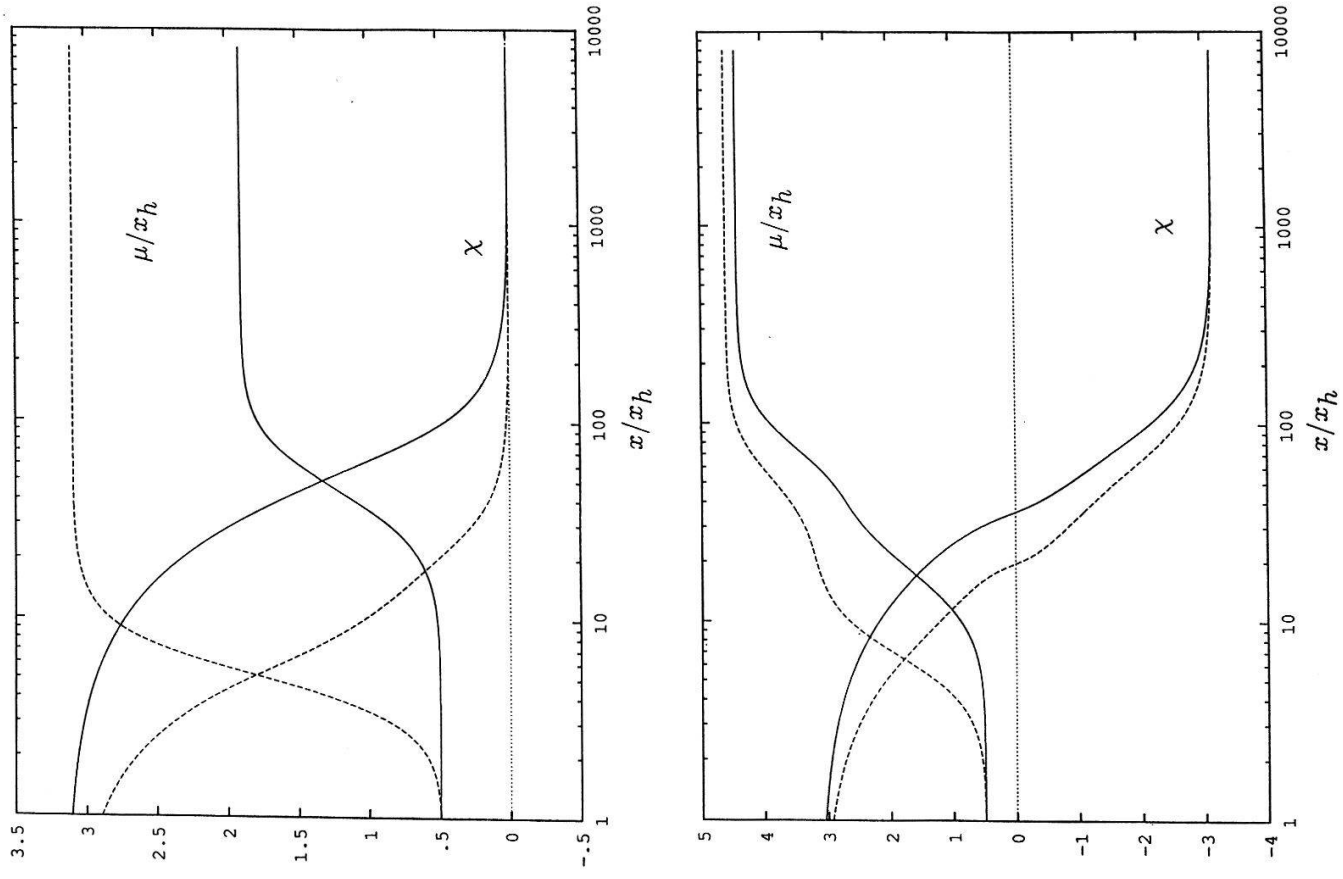

Figure 1
Hedgehog field χ and dimensionless mass function μ (in units of the horizon distance x_h) in terms of x/x_h ($\kappa = 0.005$, $x_h = 0.02$) in the first (a) and second (b) topological sector. The solid lines represent the solutions of the lower energy branches and the dashed lines the ones of the branches with higher energy.

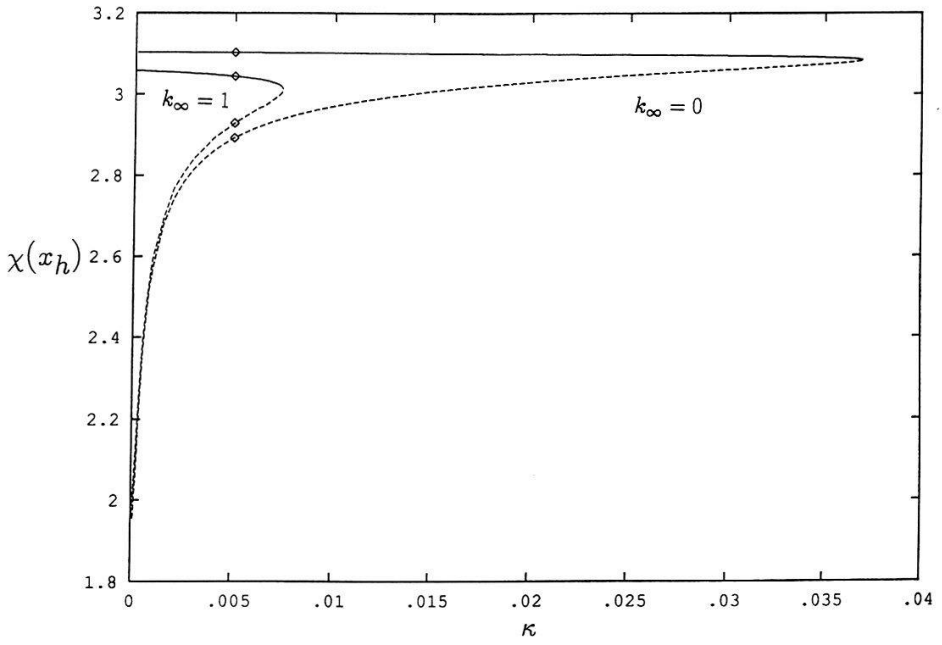

Figure 2
"Shooting parameter" $\chi(x_h)$ as a function of the dimensionless coupling constant κ in the first ($k_\infty = 0$) and second ($k_\infty = 1$) topological sector. The solid lines represent the stable black hole solutions (lower energy branches) and the dashed lines the unstable ones (higher energy branches). The squares mark the positions of the solutions plotted in Fig. 1.

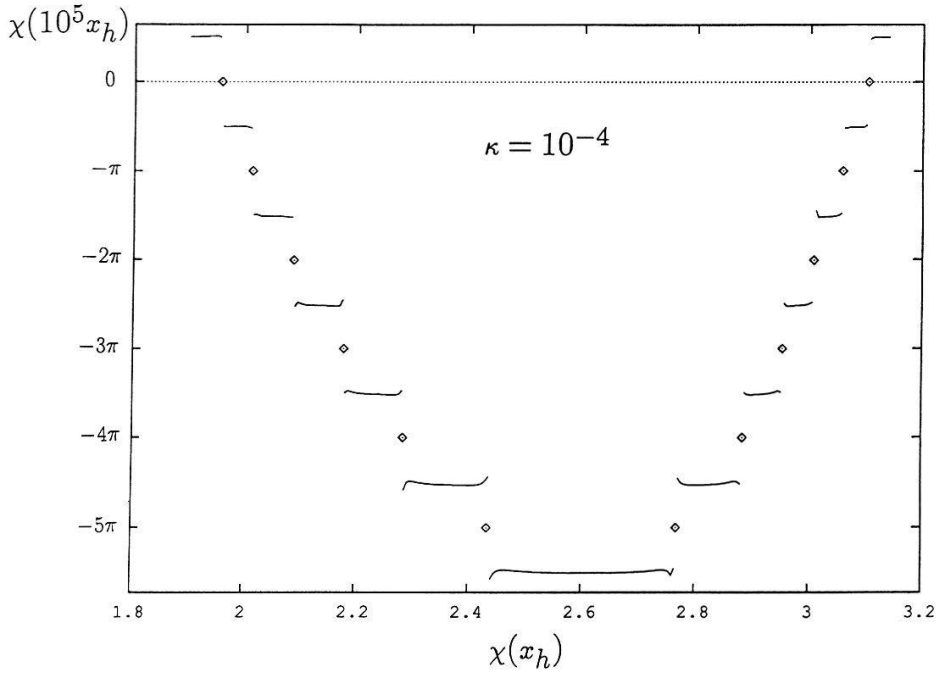

Figure 3
"Asymptotic" ($x = 10^5 x_h$) value of χ as a function of $\chi(x_h)$ for a small coupling constant ($\kappa = 0.0001$, $x_h = 0.02$). The squares represent the discrete set of asymptotically flat black hole solutions. The generic solutions do either not reach the asymptotic regime or approach odd multiples of $\pi/2$ as $x \to \infty$.

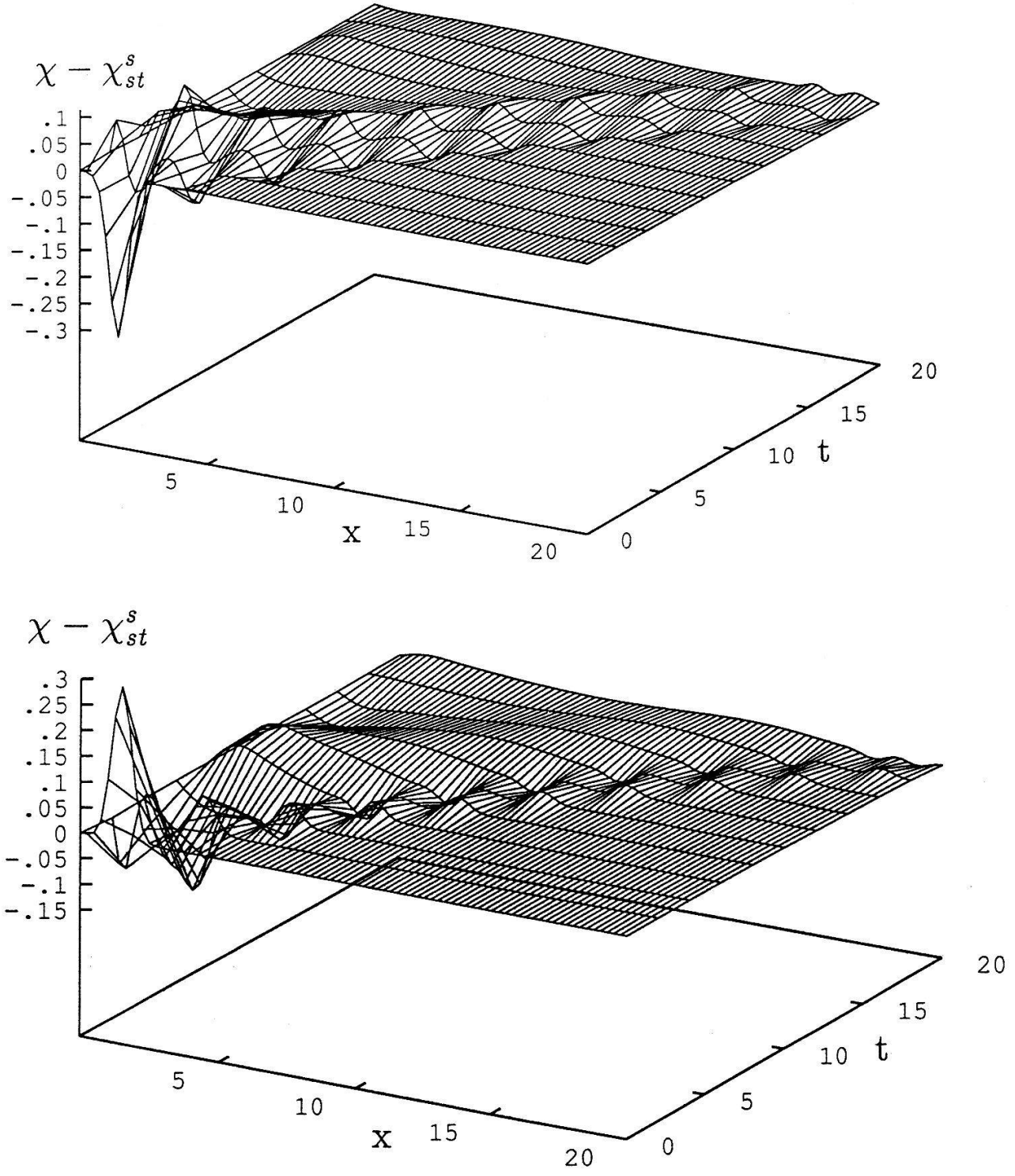

Figure 4
Time developements of perturbed solitons ($\kappa = 0.02$). The differences $\chi(x,t) - \chi^s_{st}(x)$ are plotted in (a) for a perturbation amplitude of $A = 0.3$ and in (b) for $A = -0.3$, respectively ($\kappa = 0.02$).

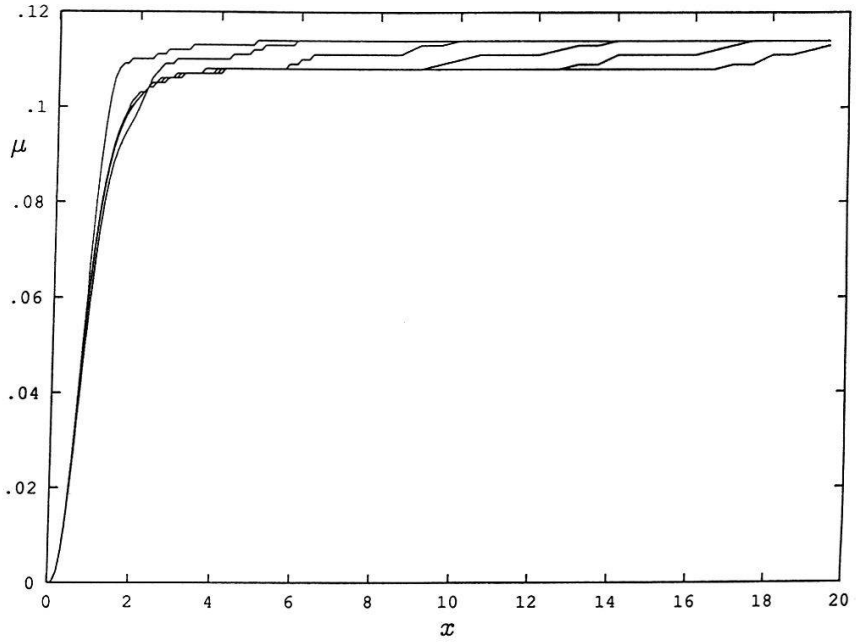

Figure 5
Mass function of the perturbed soliton ($\kappa = 0.02$) at different times. The time increment is 4. The amplitude A of the initial perturbation is $A = -0.3$.

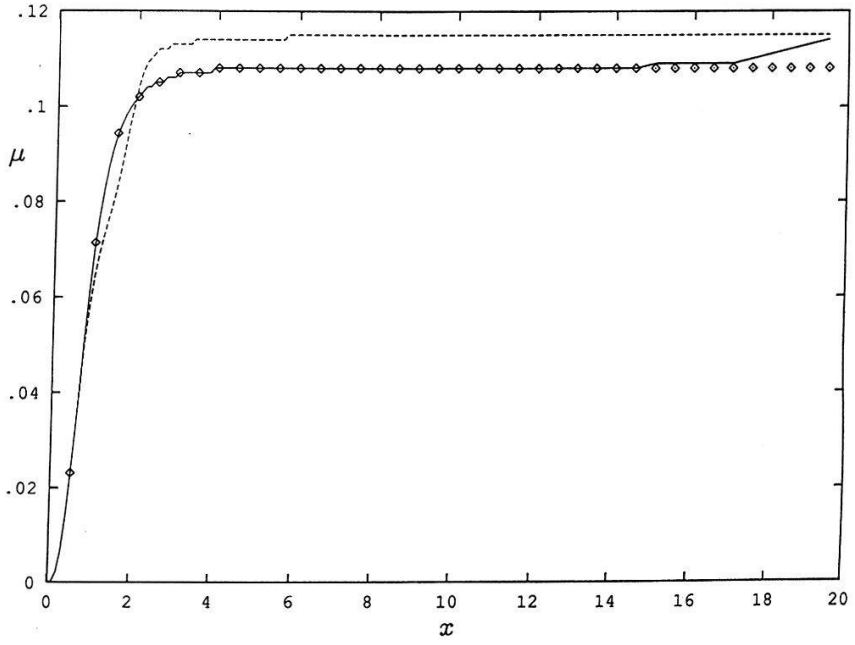

Figure 6
Mass function of the perturbed soliton ($\kappa = 0.02$) at initial and late times. The dashed line corresponds to $t = 0$ and the solid line to $t = 20$. The squares show the static mass function with $\kappa = 0.02$. The perturbation amplitude is $A = 0.3$.

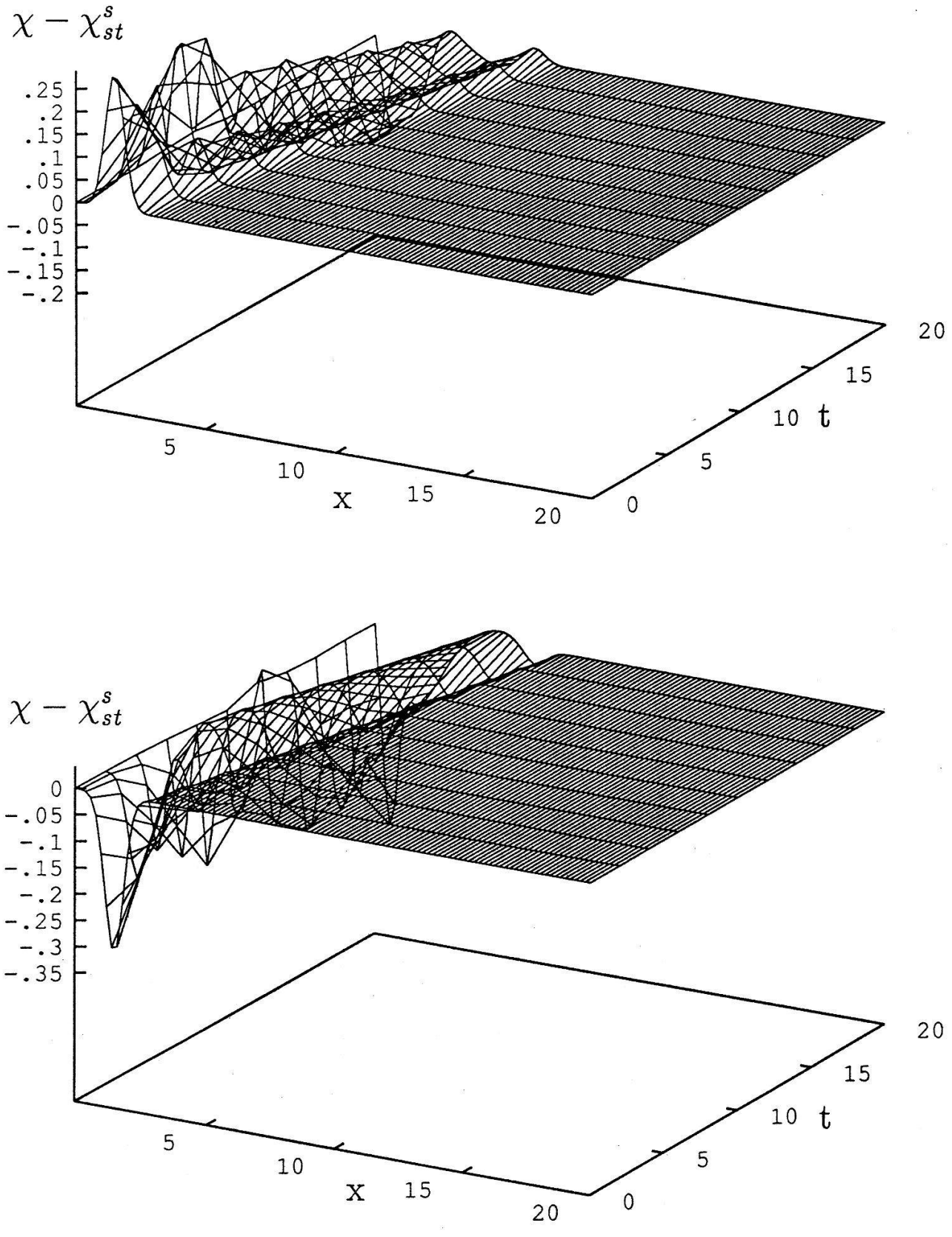

Figure 7
Evolution of the perturbed soliton ($\kappa = 0.04$). In (a) the amplitude of the initial perturbation is $A = 0.3$ and in (b) $A = -0.3$.

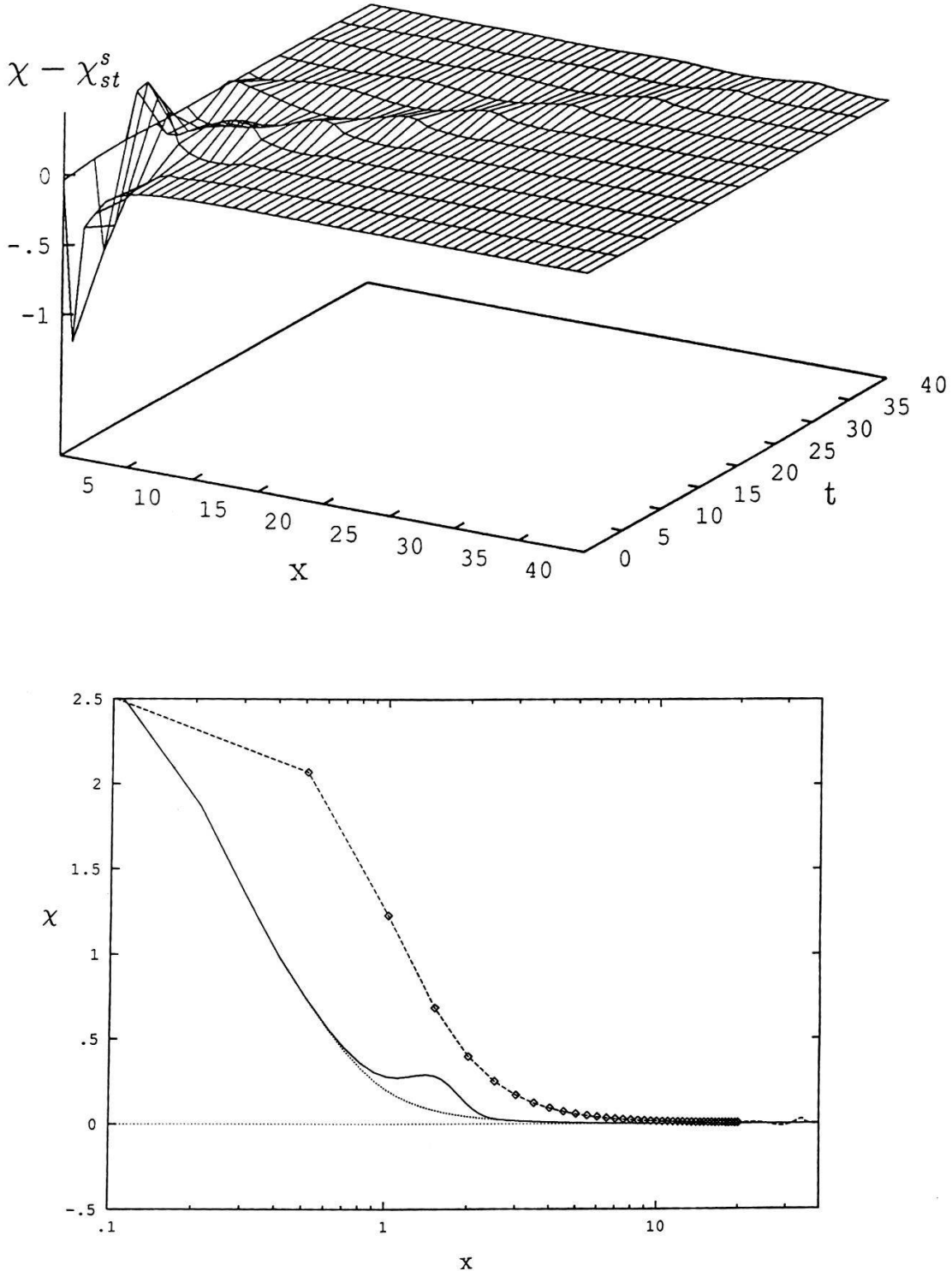

Figure 8
Evolution of the unstable soliton ($\kappa = 0.02$) under a typical perturbation. The initial amplitude of the perturbation is $A = 0.2$. In (a) $\chi(t) - \chi^s_{st}$ is shown. In (b) the perturbed χ at $t = 0$ (solid line) and at $t = 40$ (dashed line) is plotted together with the unstable soliton χ^u_{St} (dotted line) and the stable soliton χ^s_{st} (squares).

References

[1] R. Bartnik and J. McKinnon, Phys. Rev. Lett. **61** (1988) 41;

[2] H. P. Künzle and A. K. M. Masood-ul-Alam, J. Math. Phys. **31** (1990) 928;

[3] M. S. Volkov and D. V. Galtsov, Sov. J. Nucl. Phys. **51** (1990) 1171;

[4] P. Bizon, Phys. Rev. Lett. **64** (1990) 2844;

[5] N. Straumann and Z.-h. Zhou, Phys. Lett. **B 237** (1990) 353;

[6] N. Straumann and Z.-h. Zhou, Phys. Lett. **B 243** (1990) 33;

[7] Z.-h. Zhou and N. Straumann, Nucl. Phys. **B 360** (1991) 180;

[8] Z.-h. Zhou, Helv. Phys. Acta **65** (1992) 767;

[9] J. A. Smoller, A. G. Wasserman, S. T. Yau and J. B. McLeod, Comm. Math. Phys. **143** (1992) 115;

[10] J. A. Smoller, A. G. Wasserman, Comm. Math. Phys. **151** (1993) 303;

[11] M. Heusler and N. Straumann, Class. Quantum Grav. **9** (1992) 2643;

[12] M. Heusler, J. Math. Phys. **33** (1992) 3497;

[13] M. Heusler, Class. Quantum Grav. **10** (1993) 791;

[14] T. H. R. Skyrme, Proc. R. Soc. **A 260** (1961) 127;

[15] T. H. R. Skyrme, J. Math. Phys. **12** (1971) 1735;

[16] S. Droz, M. Heusler and N. Straumann, Phys. Lett. **B 268** (1991) 371;

[17] M. Heusler, S. Droz and N. Straumann, Phys. Lett. **B 271** (1991) 61;

[18] M. Heusler, S. Droz and N. Straumann, Phys. Lett. **B 285** (1992) 21;

[19] J. M. Bardeen, B. Carter and S. W. Hawking, Commun. Math. Phys. **31** (1973) 161;

[20] O. B. Zaslavskii, Phys. Lett. **A 168** (1992) 191;

[21] M. Heusler and N. Straumann, Max-Planck-Inst. prepr. MPA **723**, Zürich Univ. prepr. ZU-TH **1/93**, to appear in Class. Quantum Grav.;

[22] E. Witten, Nucl. Phys. **B 223** (1983) 422, 433;

[23] N. Pak and H. C. Tze, Ann. Phys. **117** (1979) 164;

[24] G. S. Adkins, C. R. Nappi and E. Witten, Nucl. Phys. **B 228** (1983) 552;

[25] T. H. R. Skyrme, Nucl. Phys. **31** (1962) 556;

[26] A. D. Jackson and M. Rho, Phys. Rev. Lett. **51** (1983) 751;

[27] B. Carter, in "General Relativity: An Einstein Centenary Survey", ed. S. W. Hawking and W. Israel, Cambridge Univ. Press, Cambridge (1979).

[28] N. Levinson, Kgl. Danske Videnskab. Selskab., Mat. Fys. Medd. **25/9** (1949);

[29] F. Calogero, "Variable Phase Approach to Potential Scattering", Academic Press, New York (1967);

[30] H. Luckock and I. Moss, Phys. Lett. **B 176** (1986) 341;